









ORIGINAL RESEARCH

Syringe irrigation in confluent canals: A sequential computational fluid dynamics assessment

Mário Rito Pereira DDS, MSc^{1,2}  | Goncalo Silva PhD³  |
 Viriato Semiao MSc, PhD⁴  | Jorge N. R. Martins DDS, MSc, PhD¹  |
 Vania Silverio PhD^{5,6}  | Paula Pascoal-Faria PhD⁷  | Isabel Duarte MSc, PhD^{8,9} |
 Nuno Alves PhD¹⁰  | António Ginjeira MD, DMD, PhD¹ 

¹Department of Endodontics, Faculdade de Medicina Dentária, Universidade de Lisboa, Lisboa, Portugal

²Egas Moniz Center for Interdisciplinary Research (CiiEM), Almada, Portugal

³IDMEC, Department of Mechatronics, Universidade de Évora, Évora, Portugal

⁴IDMEC, Instituto Superior Técnico, Departamento de Engenharia Mecânica, Universidade de Lisboa, Lisboa, Portugal

⁵Instituto de Engenharia de Sistemas e Computadores – Microsistemas e Nanotecnologias, INESC MN, Lisboa, Portugal

⁶Department of Physics, Instituto Superior Técnico, Universidade de Lisboa, Lisboa, Portugal

⁷Mathematics Department of the School of Technology and Management (ESTG) and Centre for Rapid and Sustainable Product Development (CDRSP) from the Polytechnic of Leiria, Marinha Grande, Portugal

⁸Department of Mechanical Engineering, Centre for Mechanical Technology and Automation (TEMA), University of Aveiro, Aveiro, Portugal

⁹LASI – Intelligent Systems Associate Laboratory, Guimarães, Portugal

¹⁰Centre for Rapid and Sustainable Product Development, Instituto Politécnico de Leiria, Marinha Grande, Portugal

Correspondence

Mário Rito Pereira, Faculdade de Medicina Dentária da Universidade de Lisboa, Rua Professora Teresa Ambrósio, Cidade Universitária, 1600-277 Lisboa, Portugal.
 Email: mariorp@campus.ul.pt

Funding information

Fundação para a Ciência e a Tecnologia; and CENTRO-01-0145-FEDER-022083; Fundação para a Ciência e Tecnologia (FCT) under LAETA; Fundação para a Ciência e Tecnologia (FCT)/BASE and PROGRAMATICO; Fundação para a Ciência e Tecnologia FCT/MCTES (PIDDAC) and Centro2020

Abstract

This study aims to assess the influence of root canal preparation, irrigation needle design and its placement depth in the irrigation flow of confluent canals during syringe irrigation. A mandibular molar presenting two confluent canals in its mesial root was sequentially prepared and scanned by micro-computed tomography after mechanical preparation up to ProTaper Next system sizes X2 (25/.06v), X3 (30/.07v) and X4 (40/.06v). In each of the root canal preparation models, a side-vented and an open-ended needle at 5, 3 and 2 mm from the working length were included, and irrigation flow was assessed by a validated computational fluid dynamics model. The results revealed that the irrigant flowed out of the confluent canals mainly through the canal that did not have the needle. Apical penetration and renewal of the irrigant were most efficiently achieved with the use of a 30G open-ended needle and a 30/.07v preparation.

KEYWORDS

computational fluid dynamics, confluent root canals, endodontics, root canal irrigation, syringe irrigation

INTRODUCTION

The effectiveness of root canal cleaning and disinfection, through irrigation, depends on the mechanical and

chemical action of the irrigants where anatomy stands as one of the main obstacles [1, 2]. The anatomical complexity, with main relevance to the apical portions of the root canal, presents a challenge for the delivery and

replenishment of irrigants in an efficient and safe way [3, 4]. This concern has been the subject of several investigations leading to the establishment of some recommendations regarding syringe irrigation [2, 5].

Computational fluid dynamics (CFD) has been used as a predictive tool to analyse the penetration and flow of the irrigants, in a given anatomy, and the influence of several clinical variables, such as the mechanical preparation size and taper [6], design and placement depth of the irrigant needle [7–9], and flow rate [10], in a relatively simple and versatile way when compared to other experimental models [11]. Most of these *in silico* research works on irrigation flow have been carried out in independent canals [6, 9, 12, 13]. However, in roots presenting multiple main canals, one of the possible and common configurations is their confluence, often identified in the mandibular molar mesial root [14]. The flow and penetration of irrigants in this configuration may lead to results different from those observed in single or independent root canals. To the best of the authors' knowledge, no data on irrigation fluid dynamics within this anatomical configuration is available.

In light of this, the aim of this study is to evaluate, in confluent root canals, the effect of different mechanical preparation size and taper combinations and two needle designs at different placement depths on the irrigant flow using a CFD model previously validated in this problem class [15].

MATERIALS AND METHODS

Root canals specimen selection and procedures

After local ethics committee approval, one two-rooted mandibular molar with two confluent mesial root canals was selected (Figure 1) from a pool of extracted teeth. The pooled specimens were examined under a clinical microscope (M320 F12; Leica MicroSystems) for root integrity, and the soft tissue remnants and calculus on the external root surface were removed by ultrasonic scaling (P5 Newtron XS; Satelec Acteon). Posteriorly, the teeth were initially scanned in a micro-computed tomography (micro-CT) device (SkyScan 1275; Bruker-micro-CT) operated at 80 kV and 125 mA, with a resolution of 19.61 μm with 360° rotation around the vertical axis, rotation step of 0.5°, camera exposure time of 58 milliseconds and frame averaging 3, using a 1-mm thick aluminium filter. The acquired projection images were reconstructed into cross-sectional slices using NRecon v.1.7.3.1 software (Bruker-micro-CT) and used to select the tooth with the initially defined anatomical parameters. Root canals had an S configuration regarding

curvature in both the clinical and proximal views. Angle measurements [16] are reported in Table 1.

Before root canal instrumentation, the molar crown was cut near the cemento-enamel junction. Working length was established at the canal terminus by inserting a 10 K-file (Dentsply Maillefer) into the canals until it was visible at the apical foramen. The glide path was done manually with 10, 15 and 20 K-file (Dentsply Maillefer). Instrumentation was conducted using ProTaper Next rotary files (Dentsply Maillefer Endodontics) following the sequence X1, X2, X3 and X4. During mechanical preparation, the irrigation was performed using 2 mL of 5.25% sodium hypochlorite (NaOCl). At the end of the preparation with each of the instruments X2 (25/.06v), X3 (30/.07v) and X4 (40/.06v), ultrasonic irrigant activation was performed for 1 min (20 s, three times), with an ultrasonic tip ISO #20 (IrriSafe; Satelec, Acteon Group) positioned 1 mm short of the working length. Two endodontic irrigation needles, a 30-G flat open-ended (NaviTip; Ultradent) and a 30-G side-vented (Max-i-Probe; Dentsply/Tulsa Dental) were placed inside the root canal to test if they could reach, without binding, the working length minus 2 mm, after each enlargement with 25/.06v, 30/.07v and 40/.06v.

The selected tooth was scanned three more times by micro-CT, after each one of the enlargements to 25/.06v, 30/.07v and 40/.06v, with the aforementioned scan setting parameters, and the acquired projection images were reconstructed into cross-sectional slices using NRecon v.1.7.3.1 software (Bruker-micro-CT).

Numerical simulation

Three 3-dimensional models of the root canals were generated, matching preparation sizes 25/.06v, 30/.07v and 40/.06v, in a Standard Template Library (STL) format file, using CTAn v.1.17.7.2 software (Bruker, micro-CT). These models were standardised to 10.4 mm in a 3D CAD software (SolidWorks 2017 x64 Edition; Dassault Systèmes), where a flat open-ended needle and a side-vented needle were designed with an outer diameter of 320 μm and an inner diameter of 170 μm based on the measurements obtained from a scanning electron microscope (Vega3-LMU; TESCAN) micrograph analysis of a 30G flat open-ended (NaviTip; Ultradent) and a 30G, side-vented, endodontic irrigation needle (Max-i-Probe; Dentsply/Tulsa Dental), respectively. The length of the needles was set to 25 mm. Based on testing conducted during the experimental work and in order to simulate only clinically realistic conditions, both needle designs were placed on the buccal root canal lumen with their apical ends positioned at 5, 3 and 2 mm short of the working length in each of the three-dimensional models.

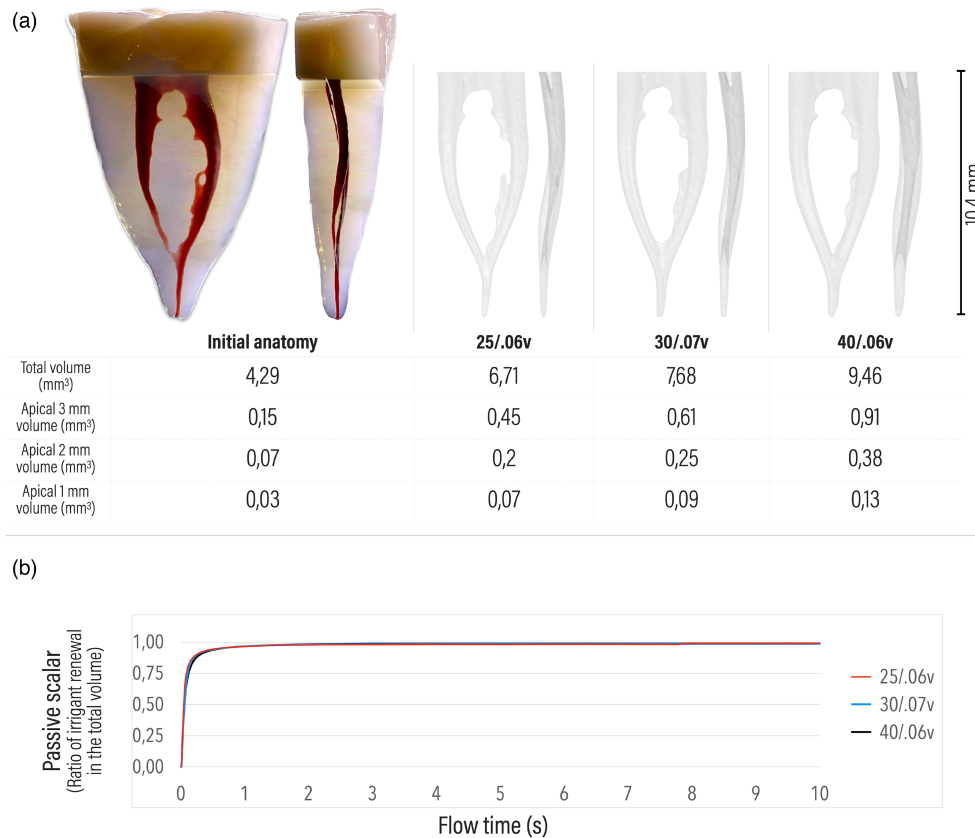


FIGURE 1 (a) Proximal and clinical view of the three-dimensional reconstruction of the mesial root and initial anatomy of the confluent root canals used in the present study, and root canals after mechanical preparation with 25/.06v, 30/.07v and 40/.06v, with their respective total and apical 3, 2 and 1 mm volume (mm³) below (from left to right). (b) Passive scalar change over time (10s) of the side-vented needle placed at 3 mm from the working length for all root canal preparations examined (25/.06v, 30/.07v and 40/.06v).

TABLE 1 Root canal curvatures measurement.

Angle	Proximal view		Clinical view	
	Lingual canal	Buccal canal	Lingual canal	Buccal canal
Coronal	25.4°	23.3°	21.5°	18.2°
Apical	14.7°	14.8°	15.3°	4.6°

These assemblies were exported to ANSYS 2019 R2 (ANSYS), where eighteen flow domains were generated, one for each combination of mechanical preparation sizes, needle types and placement depths mentioned. Tetrahedral unstructured meshes, with prism layers in the near-wall region and appropriate near-wall refinement, were created using the ANSYS Workbench meshing pre-processing module. Mesh independency tests were made until reaching the final mesh generation. Depending on the mechanical preparation size model, needle type and placement depth, final meshes contained approximately 2.2–3.2 million elements. The numerical modelling of the flow employed the ANSYS Workbench Fluent solver module, where a three-dimensional, incompressible, pressure-based transient solver was used. Continuity

equation, momentum equations and the advective-transport equation for a passive tracer were solved. The flow was considered laminar and no turbulence model was employed according to the numerical model previously validated [15].

A velocity inlet boundary condition was applied at the inlet of the needle, with a plug velocity profile matching the inlet flow rate of 0.1 mL/s. The fluid used in the CFD numerical simulations was NaOCl 2.5%, and it was modelled as an incompressible Newtonian fluid with density $\rho = 1060 \text{ kg/m}^3$ and viscosity $\mu = 1.073 \times 10^{-3} \text{ Pa}\cdot\text{s}$ [17]. The flow domain was filled with NaOCl at the starting point of the simulation. During the simulation, NaOCl solution was introduced through the needle inlet representing a ‘fresh’ NaOCl irrigant solution entering the flow domain.

In order to trace the exchange of the 'old' NaOCl solution with the 'fresh' one inside the flow domain during the irrigation process, a passive tracer scalar was defined where 0 represented the 'old' solution and 1 the 'fresh' irrigant. The molecular diffusion coefficient for both solutions was set to 0 in order to eliminate mass diffusion effects, focusing on the effects of the advective transport for the irrigant renewal only. Atmospheric pressure was imposed at both canal outlets, while canal walls were set as rigid and impermeable surfaces where the no-slip velocity boundary condition applies.

The SIMPLE algorithm was used for the pressure-velocity coupling. Second-order discretisation schemes were used for the spatial discretisation of the velocity and scalar transport equations. The convection term in the momentum equation used a second-order upwind scheme. The simulations started considering an initial resting state ($u=0$) and a uniform gauge pressure field ($p=0$) for the fluid inside the simulation domain. For the time discretisation, a bounded second-order implicit discretisation scheme was used with a $10\mu\text{s}$ time step for a real flow time simulation of 1 s. Previously, three simulations with a real flow time of 10 s were carried out for the side-vented needle placed at 3 mm from the working length in all root canal preparations (25/.06v, 30/.07v and 40/.06v) for flow time assessment purposes. The solver stopped for a convergence criterion of 0.001 in the residues of all simulated flow variables.

At the end of the simulations, the CFD-Post module was used as a post-processing tool to obtain the results and data on the irrigant replacement percentage rates, through the ratio provided by the scalar, within the total volume and at the apical 3, 2 and 1 mm volumes. For each flow domain, apical pressure, flow patterns and wall shear stress were also stored and analysed. A workstation with a 24-core Intel Xeon 2.4 GHz processor (Intel) and internal memory of 128 GB was used for the numerical simulation.

RESULTS

Changes in the total volume and apical 3, 2 and 1 mm volumes following instrumentation to size 25/.06v, 30/.07v and 40/.06v are reported in [Figure 1a](#).

The results of the three simulations carried out for the purpose of flow assessment time presented in [Figure 1b](#) show the passive scalar change over 10 s of simulation time of the side-vented needle placed at 3 mm from the working length for all the root canal preparations examined. Starting from a rest situation, it undergoes a short transient period where the most significant changes in irrigation renewal were recorded in the first 0.5 s in all cases. Thereafter, it attained a relatively stable exchange

condition, with variations of <2% between the first and tenth seconds, reaching a 'quasi-steady state'.

Flow pattern

The flow pattern resulting from the irrigant injection is displayed in the form of vectors along the streamlines in [Figure 2](#). As it can be observed, both needles generate slightly different jets after their outlets. After this jet, the flow is directed to the root canal orifices, mainly through the confluent canal opposite to the one containing the needle. This behaviour is observed regardless of the needle outlet being located coronal or apical to the confluence of the root canals. Additionally, increasing root canal preparation, following the sequence of the instrumentation system employed, does not promote a relevant change in this pattern ([Figure 2](#)).

Irrigant replenishment and penetration

[Figure 3](#) displays the irrigant penetration and renewal of the apical 3, 2, 1 mm and total root canal volumes. It can be seen that, overall, high rates of irrigant renewal were obtained in the total volume of the root canals.

The apical 3 mm registered differences for all preparation sizes and placement depths with the side-vented needle. Irrigant is unable to fully reach the working length at any size or placement depth for that needle type. The best scenarios for the side-vented needle, regarding apical penetration and irrigant renewal, are seen when its apical limit is positioned 2 mm short of the working length with 25/.06v root canal preparation and at any placement depth with 40/.06v preparation. For the studied file sequence, root canal enlargement enhanced irrigant renewal and penetration at the apical 3 mm for the same side-vented needle placement length, excluding the enlargement from a 25/.06v to a 30/.07v preparation when the needle is placed 2 mm from the WL. There are no major differences between the different side-vented needle placement depths within the same mechanical preparation file, except for the 25/.06v when the needle is placed 2 mm short of the working length ([Figure 3](#)).

With the open-ended needle, as opposed to the side-vented needle, irrigant penetration is almost able to reach the working length in all situations except with root canal preparation 25/.06v with the needle positioned at 3 and 5 mm short of the working length. Needle placement depth has a direct relationship in the improvement of apical penetration and irrigant renewal, with a 25/.06v preparation. Apart from these two cases, the renewal of

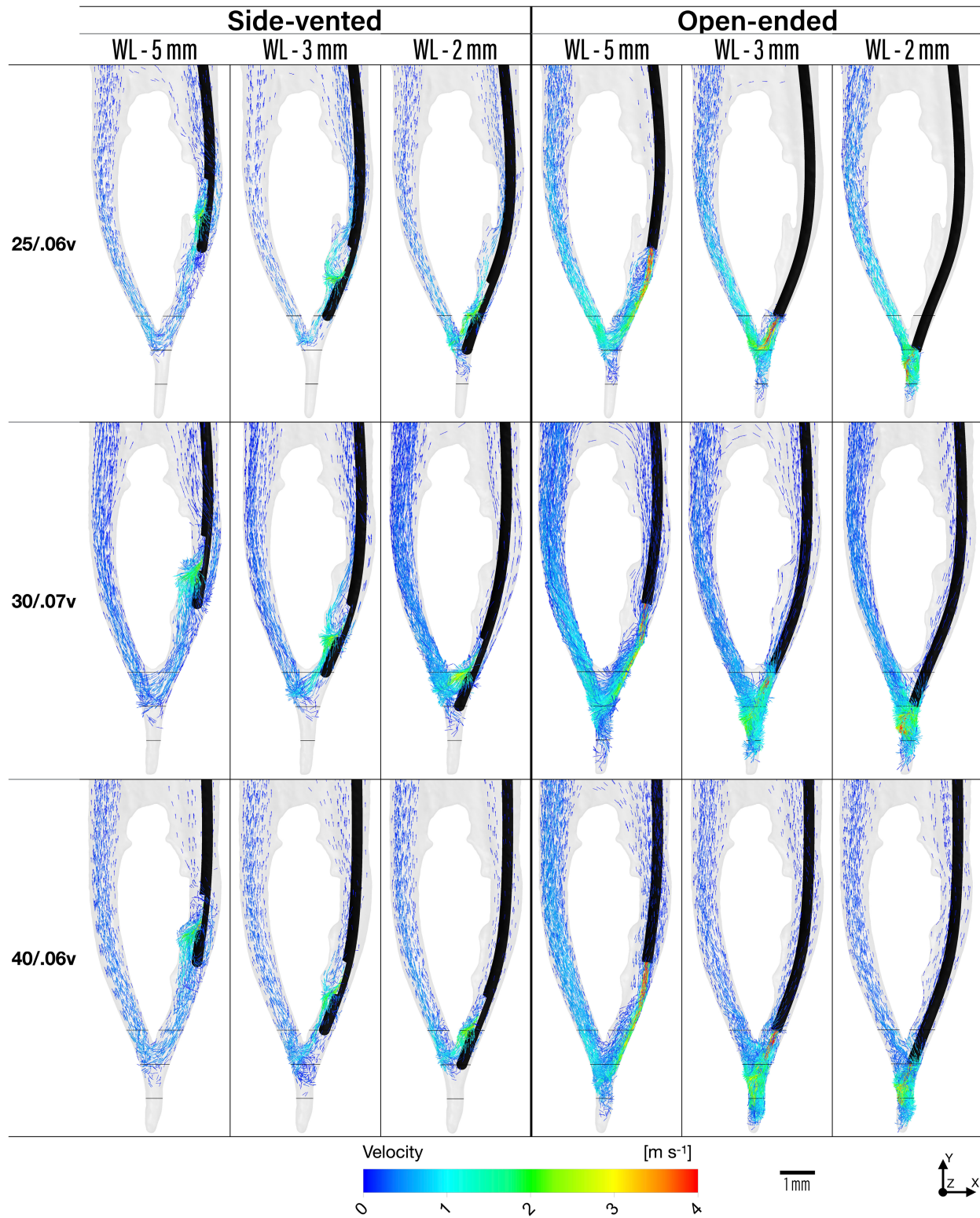


FIGURE 2 Velocity vectors along the streamlines showing the direction of massless particles inside the root canal coloured according to the velocity magnitude (at $t=1$ s) for the side-vented needle and open-ended needle placed at the working length (WL) minus 5, 3, 2 mm in all root canal preparations assessed (25/.06v, 30/.07v and 40/.06v).

the irrigant is almost complete in all 3 mm apical volume. No differences are observed between 30/.07v and 40/.06v root canal preparations, where the placement depth of the open-ended needle has no influence on irrigant

penetration and renewal. Also, the irrigant replenishment in the coronal and middle thirds of the root canals seems to have improved with the root canal enlargement to 30/.07v. (Figure 3).

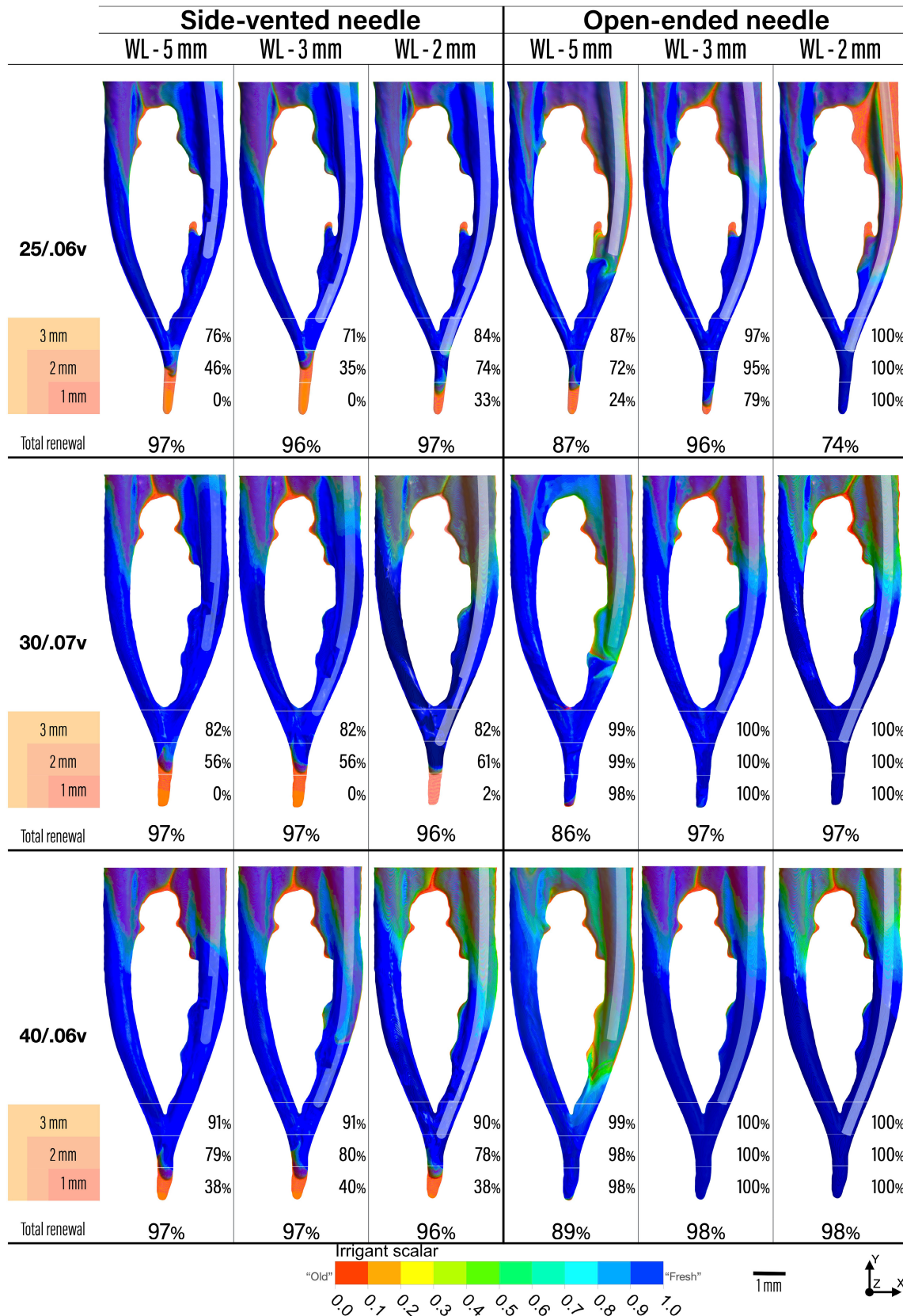


FIGURE 3 Irrigant penetration and renewal of the 3, 2, 1 mm and total volume (at $t = 1$ s) for the side-vented needle and open-ended needle placed at the working length (WL) minus 5, 3, 2 mm in all root canal preparations assessed (25/.06v, 30/.07v and 40/.06v).

The irrigant penetration beyond the needles tip increases proportionally to the distance of the needle to the working length, with the preparation size and with the use of open-ended needle related to the side-vented needle.

Apical pressure

Figure 4 shows the generated apical pressure, which is always higher for the open-ended needle case. For both needles, the apical pressure increases when the needle is placed closer to the working length. When considering an identical depth of the needle apical tip positioning, an increase in root canal preparation tends to result in a slight decrease of apical pressure.

Wall shear stress

The shear stress on the root canal walls is confined to an area near the needle outlet, where it registers the maximum values (Figure 5). With the side-vented needle this area is limited to the wall facing the outlet whereas with the open-ended needle it spreads towards the root canal walls circumferential and apically to the needle tip. The maximum time-averaged values for the wall shear stress range from 1700 to 184 N/m^2 for the side-vented needle and from 1283 to 130 N/m^2 for the open-ended needle. Considering the same needle and placement depth, the

increase in the root canal preparation leads to lower wall shear stress values. Regarding the maximum time-averaged values for wall shear stress, no trend is observable for both the design and the placement depth of needles.

DISCUSSION

Using a previously validated CFD model [15], the present research assessed the effect of several parameters on the irrigant penetration and flow within confluent root canals of a mandibular mesial root. The mechanical and chemical effect of the irrigants on pulp tissue remnants, microorganisms, biofilm, hard tissue debris and smear layer can only take place if the irrigants are able to contact those components. Additionally, the renewal of NaOCl solutions in all areas of the root canal system is crucial to maintain its chemical properties due to its rapid depletion [18]. The use of the advective transport of a passive scalar in this investigation was the method employed to both directly visualise the three-dimensional renewal extension and associated boundaries, and to quantify these parameters for a more comprehensive assessment of the irrigant replacement.

Due to the dimensions of the root canals, physical characteristics and flow rate of the irrigants, the steady state establishment of the physical variables, such as velocity and pressure, is a very fast phase that can take less than 0.2s starting from a resting state as reported in previous

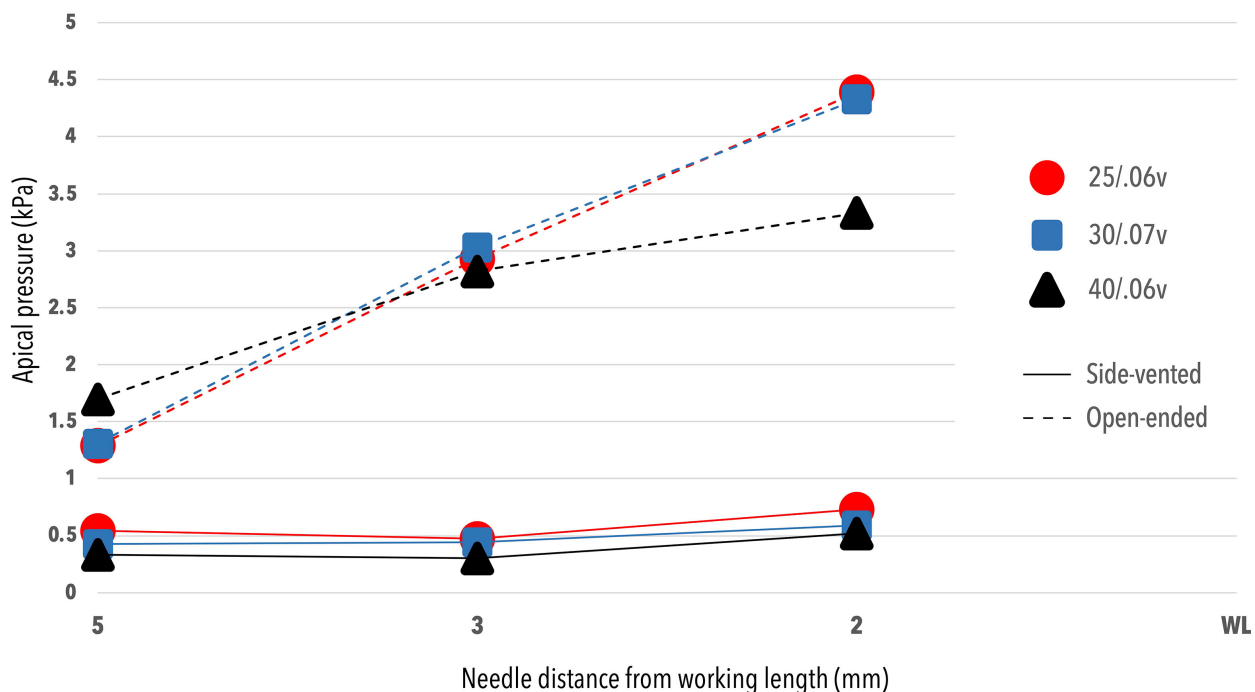


FIGURE 4 Time-averaged pressure at the apical end of the root canal as a function of the needle distance from the working length, for the side-vented needle, open-ended needle and root canal preparations 25/.06v, 30/.07v and 40/.06v.

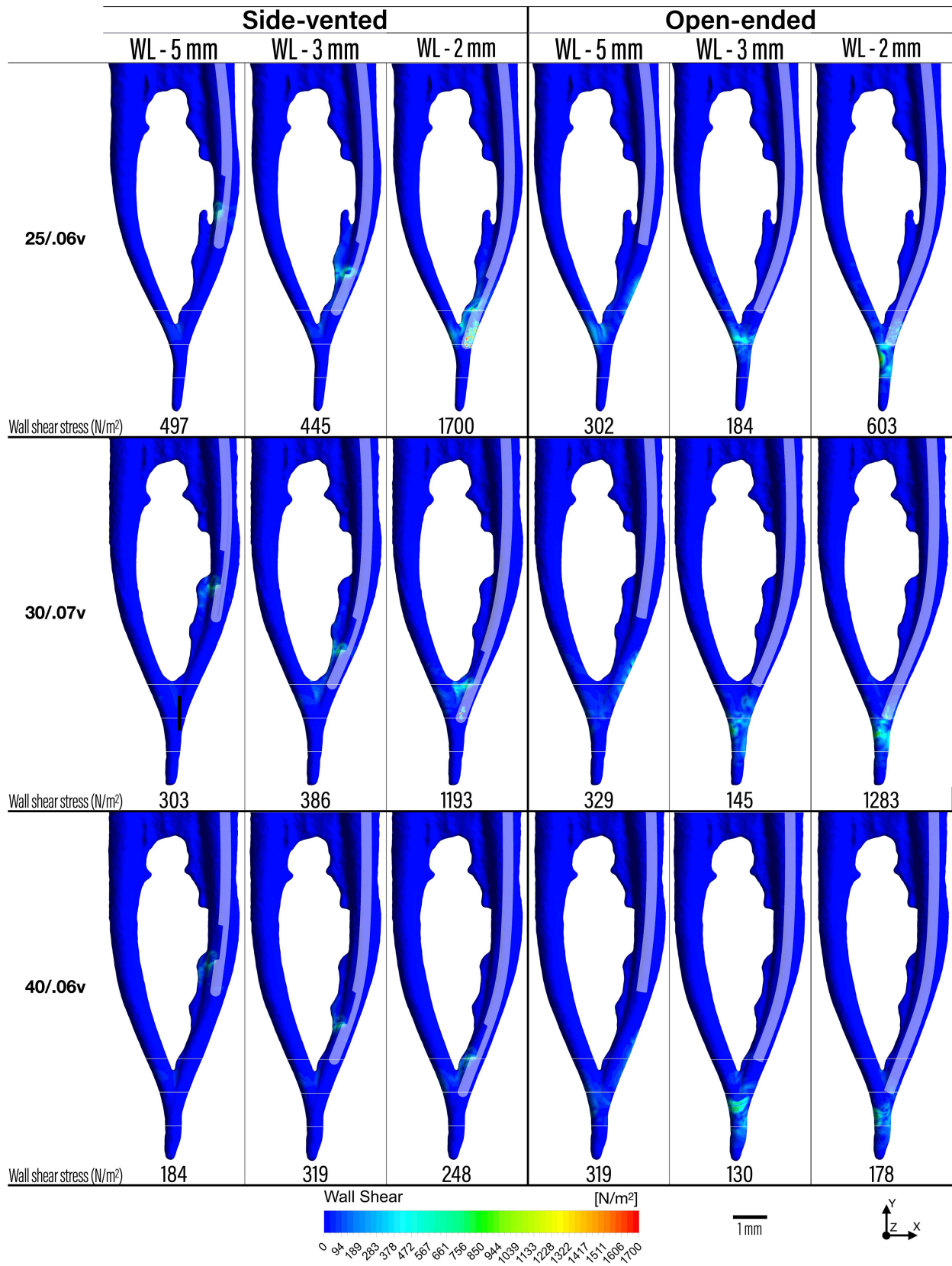


FIGURE 5 Contours and maximum time-averaged wall shear stress (N/m²) for all cases studied for the side-vented needle and open-ended needle placed at the working length (WL) minus 5, 3, 2 mm in all root canal preparations assessed (25/.06v, 30/.07v and 40/.06v).

experimental validation [15]. However, the use of the additional passive scalar, used in the present research to represent irrigant replacement, could have a different performance, and therefore, a prior assessment of its behaviour over time was required. The results on the evolution of the advective transport of the passive scalar displayed a transient behaviour in all cases. The small variation of irrigant replacement after the first second, that takes place in areas where the velocity is very low, has already been reported [19]. For this reason, associated with the high computational cost of CFD simulations, this assessment was carried out using a transient simulation with a time period of 1 s, after which the irrigant renewal percentage is expected to increase very slowly and residually, not only due to the reported convective transport but also for the molecular diffusive transport. From a clinical perspective, the irrigation time can often reach 5–10 s, sometimes even longer [20], which also increases the mechanical effect of the irrigant flow through advection and wall shear stress effects.

The high rates of irrigant renewal seen in the present investigation during the 1 s simulation timeframe are consistent with earlier findings [19]. No conclusions were drawn about the effect of the increase in root canal preparation on the anatomical features and irregularities in the main root canal walls since mechanical preparation led to small changes between each of the preparation 3D models (Figure 1) due to the accumulation or removal of hard tissue debris from these areas, despite the use of ultrasonics prior to the micro-CT scans [21, 22] and/or by decreasing the lumen of these areas due to the enlargement of the canal. The use of ultrasonics in the present investigation and the potential creation of defects on the walls of the main root canals were considered and assessed in a previous pilot study, where the detrimental effect of debris accumulation on the differences between mechanical preparation models was much greater than the controlled use of ultrasonics. Although this can be considered a limitation of this study, at the same time, it reflects and should be taken into account within a clinical setting. Nevertheless, depending on the needle design and placement depth, the irrigant was able to penetrate these anatomical features and irregularities in each mechanical preparation to different extents. This supports the assumption that the inward and outward movement of the needle may enhance the penetration of the irrigant into these areas by adding up these different penetration extents. However, in areas of smaller diameter and thickness such as fins, renewal appeared to be compromised for all situations assessed in the present study. This observation has been documented in previous studies [23, 24] and a correlation between irrigant velocity and the removal of biofilms in these anatomical features has already been established [25] showing that in these unprepared areas,

where the velocity is extremely low or nil, no chemical or mechanical effect takes place and cleaning and disinfection is compromised as seen in correlative studies [26, 27].

In regard to apical irrigant penetration and renewal, each needle type produced different results. The inability of the irrigant to reach the working length with the side-vented needle in the confluent canals investigated in this study is in line with that reported for independent canals [6]. The characteristic flow pattern generated with this needle design limits its apical penetration when compared with open-ended needles [28]. However, in this type of anatomy, the presence of an additional canal to the one containing the needle, as well as the coronal position of the side-vented needle outlet related to the canals' confluence, seems to have an important influence in constraining the apical penetration of the irrigant to the working length. The fact that most of the irrigant exited the root canal system through the canal opposite to the one with the needle, as seen in the generated flow patterns (Figure 2), seems to have influenced the overall lack of differences in irrigant renewal and apical penetration for the different side-vented needle placement depths within the same root canal preparation. The increase in the mechanical preparation sequence has tended to enhance renewal rates and irrigant apical penetration, like that seen in independent canals in previous studies [12, 29].

The open-ended needle favours irrigant penetration to the working length, as such penetration is almost attained in the majority of scenarios studied. The exception is for the 25/.06v preparation case when the needle is placed at 5 and 3 mm from the working length, although in the latter case the renewal rate is high in the apical millimetre. This inability of apical irrigant penetration to the working length in preparations with an apical preparation of 25/.06 is consistent with other studies using numerical models in independent canals [6, 12]. In practice this can result in a reduced chemical and mechanical action of the irrigants compared to larger apical sizes, as results of a previous clinical investigation regarding bacterial reduction suggests [30]. However, with the enlargement to the 30/.07v preparation, the penetration and apical renewal of the irrigant reached optimal rates regardless of needle placement depth. Increasing the preparation to 40/.06v did not provide any additional benefits for the open-ended needle.

In addition to irrigant penetration and renewal within the root canal system space, which are critical to irrigation chemical effect, wall shear stress, a physical fluid dynamics quantity provided with this numerical model analysis, is employed as a surrogate for the irrigation mechanical effect [6, 31]. It is observed that the maximum values of wall shear stress tend to decrease as mechanical preparation increases. This pattern was already identified in previous studies [12, 29] and is explained by the increased

distance between the needle outlet and the root canal walls. As variables dependent on the needle outlet and its proximity to the root canal walls, the anatomical irregularities and confluence zone present in the anatomical models studied can explain the relatively uncorrelated results. As seen previously for irrigant penetration, this is another effect that might be enhanced with the inward and outward movement of the needle, as recommended by some authors [5, 32].

Beside irrigant renewal and apical penetration, safety concerns must always be considered during positive pressure irrigation. The generated apical pressure data is used to determine the relative risk of irrigant extrusion since, aside from not being the primary determinant, there is no reference value from which a hypochlorite accident is known to occur. In the present study, the changes in apical pressure follow the trends previously documented for independent canals [7, 12, 29]. Several studies using the same flow rate, needle placement depth and design report some divergences in the generated apical pressure [8, 9, 19]. Differences in anatomy and the use of a CFD model assuming a turbulent flow might be the reasons for such divergence, adding to the fact that none of these studies validated the employed numerical model.

Combining the data of apical pressure and irrigant penetration for the side-vented needle, we can state that, while it registers relatively low values and little likelihood of promoting irrigant extrusion, it is ineffective in the renewal and delivery of irrigants to the working length within the root canal anatomy studied herein. The recommended placement of the side-vented needle within 1 mm of the working length [33] could improve the scenario, but the anatomy might not always permit it, as in the case evaluated in this study. The use of 31 G needles could be an alternative to overcome this issue [6]. The open-ended needle generates the highest apical pressure and a larger risk of irrigant extrusion when compared with the side-vented needle and when placed closest to the working length and for all preparation sizes, but on the other hand, it shows high efficiency in the delivery of the irrigant to the working length at any of the placement depths studied, suggesting its placement at 3 mm or even 5 mm, except for 25/.06v preparation where the relation between irrigant penetration and apical pressure seemed to be more balanced when placed 3 mm short of the working length.

Regarding the effect of enlarging the root canal with the sequence of files used, the results are different depending on the type of needle used. While with the open-ended needle no major benefits are observed with root canal enlargement to 40/0.06v, as renewal and penetration extend almost entirely to the WL at 30/.07v, with the side-vented needle, although never reaching the WL, the

root canal enlargement led to an improvement in irrigant renewal and apical penetration for all mechanical preparations evaluated, with the exception of the increase from 25/.06v to 30/.07v when the needle is located 2 mm from the WL, a finding that contradicts the general trend reported in the manuscript and in earlier studies [12, 29]. From the generated flow pattern results, it can be seen that in preparation 30/.07v, when the side-vented needle is placed 2 mm from the WL, the flow is more concentrated and directed towards the canal opposite to the one with the needle, compared to preparations 25/.06v and 40/.06v, which seem to limit the apical penetration of the irrigant, leading to this contradictory finding. The reasons for this seem to lie in the fact that the root canal enlargement led to an increase in the canal lumen not only apically but also in the canal opposite the needle, providing more space for the flow towards the exit, combined with the fact that the confluence zone in preparation 30/.07v had a configuration that allowed the jet generated from the side-vented needle to be more directed towards the canal opposite the needle and, therefore, to the exit. This change in the confluence zone between the evaluated root canal preparations was due not only to the shaping provided by the root canal instrumentation but also to the accumulation and removal of debris, which, as previously discussed, resulted in these small changes between the root canal preparation sizes and their respective 3D models, something that, although minimised, cannot be completely eliminated either in the use and preparation of real root canal anatomy for this type of research or in a real clinical scenario [21, 22]. Taken together, the gains in apical irrigant penetration by opting for an open-ended needle appear to be greater than the root canal enlargement for a 40/.06v preparation in the anatomy assessed in this study. These remarks and results should be interpreted with caution, as this study aimed to evaluate the flow generated with syringe irrigation within this specific anatomy. A more coronal or apical confluence zone than the one evaluated in this research could modify the results obtained regarding apical penetration and needle type, and it is important to assess their influence in future studies. Additionally, in a clinical setting, other factors must also be considered, and each root canal anatomy with a different preoperative morphology would require a different final shape and apical preparation in order to avoid structural weakening or preparation errors [34]. Also, these results were obtained for the combined effect of tip size and taper specific to the variable-taper rotary instruments used. The effect of different combinations of size and taper, as well as their isolated effect on this type of anatomy, should be addressed in future studies to evaluate their influence on the flow, as already shown for independent canals [6, 12, 29].

In the present study, the sequential assessment of the root canal preparation combined with the needle design and its proximity to the working length provided a correlation and evaluation of their influence in the irrigant flow of confluent canals. The flow rate is another known parameter influencing the irrigation flow [6, 10], which was kept constant and with a value of 0.1 mL/s in the current research. This flow rate is a clinically realistic value [20] and a potentially usable higher flow rate must first be experimentally validated for this anatomic configuration. Future research using other anatomical configurations is crucial to better understand and assess the differences in irrigant flow, such as those recorded in the confluent canals studied in this research and independent canals from previous studies.

CONCLUSIONS

As a conclusion, in the confluent canal anatomy studied in this investigation, the apical penetration of NaOCl is not able to fully extend to the working length with the use of a 30G side-vented needle in any of the studied preparation sizes. With the use of a 30G open-ended needle, this penetration is almost possible even with a 25/.06v preparation and when placed 2 mm short of the working length, although with an increased risk of extrusion. Increasing to 30.07 v allows irrigant penetration almost up to the working length for all open-ended needle placement depths investigated, as well as lower apical pressure. No substantial benefits are seen from enlarging the root canal to size 40/.06v.

AUTHOR CONTRIBUTIONS

All authors have contributed significantly and are in agreement with the manuscript.

ACKNOWLEDGEMENTS

This work was supported by FCT, through IDMEC, under LAETA, project UIDB/50022/2020. Research Unit INESC MN (UID/05367/2020) acknowledges FCT funding through plurianual BASE and PROGRAMATICO. This research was financially supported by the Fundação para a Ciência e a Tecnologia FCT/MCTES (PIDDAC) and Centro2020 through the following Projects: UIDB/04044/2020; UIDP/04044/2020; Associate Laboratory ARISE LA/P/0112/2020; PAMI - ROTEIRO/0328/2013 (No 022158) and FCT Project OptiBioScaffold - PTDC/EMESIS/4446/2020. The authors acknowledge the support by the projects UIDB/00481/2020 and UIDP/00481/2020 - Fundação para a Ciência e a Tecnologia; and CENTRO-01-0145-FEDER-022083 - Centro Portugal Regional Operational Programme (Centro2020), under the PORTUGAL 2020 Partnership Agreement, through the European Regional Development Fund.

CONFLICT OF INTEREST STATEMENT

The authors deny any conflicts of interest.

ORCID

Mário Rito Pereira  <https://orcid.org/0000-0002-1632-5809>
 Gonçalo Silva  <https://orcid.org/0000-0001-5719-799X>
 Viriato Semiao  <https://orcid.org/0000-0003-0612-8155>
 Jorge N. R. Martins  <https://orcid.org/0000-0002-6932-2038>
 Vania Silverio  <https://orcid.org/0000-0002-8368-3374>
 Paula Pascoal-Faria  <https://orcid.org/0000-0003-1474-9496>
 Nuno Alves  <https://orcid.org/0000-0002-5016-0868>
 António Ginjeira  <https://orcid.org/0000-0001-5114-1426>

REFERENCES

1. Haapasalo M, Endal U, Zandi H, Coil JM. Eradication of endodontic infection by instrumentation and irrigation solutions. *Endod Topics*. 2005;10:77–102.
2. Zehnder M. Root canal irrigants. *J Endod*. 2006;32:389–98.
3. Park E, Shen Y, Haapasalo M. Irrigation of the apical root canal: irrigation of the apical root canal. *Endod Topics*. 2012;27:54–73.
4. Zhu W, Gyamfi J, Niu L, Schoeffel GJ, Liu SY, Santarcangelo F, et al. Anatomy of sodium hypochlorite accidents involving facial ecchymosis – a review. *J Dent*. 2013;41:935–48.
5. Boutsoukias C, van der Sluis LWM. Syringe irrigation: blending endodontics and fluid dynamics. In: Basrani B, editor. *Endodontic irrigation: chemical disinfection of the root canal system*. Cham, Switzerland: Springer; 2015. p. 45–64.
6. Boutsoukias C, Nova PG. Syringe irrigation in minimally shaped root canals using 3 endodontic needles: a computational fluid dynamics study. *J Endod*. 2021;47:1487–95.
7. Boutsoukias C, Lambrianidis T, Verhaagen B, Versluis M, Kastrinakis E, Wesselink PR, et al. The effect of needle-insertion depth on the irrigant flow in the root canal: evaluation using an unsteady computational fluid dynamics model. *J Endod*. 2010;36:1664–8.
8. Loroño G, Zaldivar JR, Arias A, Cisneros R, Dorado S, Jimenez-Octavio JR. Positive and negative pressure irrigation in oval root canals with apical ramifications: a computational fluid dynamics evaluation in micro-CT scanned real teeth. *Int Endod J*. 2020;53:671–9.
9. Shen Y, Gao Y, Qian W, Ruse ND, Zhou X, Wu H, et al. Three-dimensional numeric simulation of root canal irrigant flow with different irrigation needles. *J Endod*. 2010;36:884–9.
10. Boutsoukias C, Lambrianidis T, Kastrinakis E. Irrigant flow within a prepared root canal using various flow rates: a computational fluid dynamics study. *Int Endod J*. 2009;42:144–55.
11. Boutsoukias C, Arias-Moliz MT, Paz LEC. A critical analysis of research methods and experimental models to study irrigants and irrigation systems. *Int Endod J*. 2022;55(Suppl 2):295–329.
12. Boutsoukias C, Gogos C, Verhaagen B, Versluis M, Kastrinakis E, van der Sluis LWM. The effect of apical preparation size on irrigant flow in root canals evaluated using an unsteady computational fluid dynamics model. *Int Endod J*. 2010;43:874–81.

13. Gao Y, Haapasalo M, Shen Y, Wu H, Li B, Ruse ND, et al. Development and validation of a three-dimensional computational fluid dynamics model of root canal irrigation. *J Endod.* 2009;35:1282–7.
14. Versiani MA, Pereira MR, Pécora JD, Sousa-Neto MD. Root canal anatomy of maxillary and mandibular teeth. In: Versiani MA, Basrani B, Sousa-Neto MD, editors. *The root canal anatomy in permanent dentition.* Cham, Switzerland: Springer; 2018. p. 181–239.
15. Pereira MR, Silva G, Semiao V, Silverio V, Martins JNR, Pascoal-Faria P, et al. Experimental validation of a computational fluid dynamics model using micro-particle image velocimetry of the irrigation flow in confluent canals. *Int Endod J.* 2022;55:1394–403.
16. Cunningham CJ, Senia ES. A three-dimensional study of canal curvatures in the mesial roots of mandibular molars. *J Endod.* 1992;18:294–300.
17. Guerisoli DMZ, Silva RS, Pecora JD. Evaluation of some physico-chemical properties of different concentrations of sodium hypochlorite solutions. *Braz Endod J.* 1998;3:21–3.
18. Moorer WR, Wesselink PR. Factors promoting the tissue dissolving capability of sodium hypochlorite. *Int Endod J.* 1982;15:187–96.
19. Wang R, Shen Y, Ma J, Huang D, Zhou X, Gao Y, et al. Evaluation of the effect of needle position on irrigant flow in the C-shaped root canal using a computational fluid dynamics model. *J Endod.* 2015;41:931–6.
20. Boutsoukis C, Lambrianidis T, Kastrinakis E, Bekiaroglou P. Measurement of pressure and flow rates during irrigation of a root canal ex vivo with three endodontic needles. *Int Endod J.* 2007;40:504–13.
21. Linden D, Boone M, Bruyne MD, De Moor R, Versiani MA, Meire M. Adjunctive steps for the removal of hard tissue debris from the anatomic complexities of the mesial root canal system of mandibular molars: a micro-computed tomographic study. *J Endod.* 2020;46:1508–14.
22. Chan R, Versiani MA, Friedman S, Malkhassian G, Sousa-Neto MD, Leoni GB, et al. Efficacy of 3 supplementary irrigation protocols in the removal of hard tissue debris from the mesial root canal system of mandibular molars. *J Endod.* 2019;45:923–9.
23. Conde AJ, Estevez R, Loroño G, Valencia de Pablo Ó, Rossi-Fedele G, Cisneros R. Effect of sonic and ultrasonic activation on organic tissue dissolution from simulated grooves in root canals using sodium hypochlorite and EDTA. *Int Endod J.* 2017;50:976–82.
24. Jiang LM, Lak B, Eijsvogels LM, Wesselink P, van der Sluis LWM. Comparison of the cleaning efficacy of different final irrigation techniques. *J Endod.* 2012;38:838–41.
25. Pereira TC, Boutsoukis C, Dijkstra RJB, Petridis X, Versluis M, de Andrade FB, et al. Biofilm removal from a simulated isthmus and lateral canal during syringe irrigation at various flow rates: a combined experimental and computational fluid dynamics approach. *Int Endod J.* 2021;54:427–38.
26. Perez R, Neves AA, Belladonna FG, Silva EJNL, Souza EM, Fidel S, et al. Impact of needle insertion depth on the removal of hard-tissue debris. *Int Endod J.* 2017;50:560–8.
27. Siqueira JF, Pérez AR, Marceliano-Alves MF, Provenzano JC, Silva SG, Pires FR, et al. What happens to unprepared root canal walls: a correlative analysis using micro-computed tomography and histology/scanning electron microscopy. *Int Endod J.* 2017;51:501–8.
28. Boutsoukis C, Verhaagen B, Versluis M, Kastrinakis E, Wesselink PR, van der Sluis LWM. Evaluation of irrigant flow in the root canal using different needle types by an unsteady computational fluid dynamics model. *J Endod.* 2010;36:875–9.
29. Boutsoukis C, Gogos C, Verhaagen B, Versluis M, Kastrinakis E, van der Sluis LWM. The effect of root canal taper on the irrigant flow: evaluation using an unsteady computational fluid dynamics model. *Int Endod J.* 2010;43:909–16.
30. Rodrigues R, Zandi H, Kristoffersen A, Enersen M, Mdala I, Ørstavik D, et al. Influence of the apical preparation size and the irrigant type on bacterial reduction in root canal-treated teeth with apical periodontitis. *J Endod.* 2017;43:1058–63.
31. Chen JE, Nurbakhsh B, Layton G, Bussmann M, Kishen A. Irrigation dynamics associated with positive pressure, apical negative pressure and passive ultrasonic irrigations: a computational fluid dynamics analysis. *Aust Endod J.* 2014;40:54–60.
32. Huang TY, Gulabivala K, Ng YL. A bio-molecular film ex vivo model to evaluate the influence of canal dimensions and irrigation variables on the efficacy of irrigation. *Int Endod J.* 2008;41:60–71.
33. Boutsoukis C, Arias-Moliz MT. Present status and future directions – irrigants and irrigation methods. *Int Endod J.* 2022;55(Suppl 3):588–612.
34. Arias A, Peters OA. Present status and future directions: canal shaping. *Int Endod J.* 2022;55(Suppl 3):637–55.

How to cite this article: Rito Pereira M, Silva G, Semiao V, Martins JNR, Silverio V, Pascoal-Faria P, et al. Syringe irrigation in confluent canals: A sequential computational fluid dynamics assessment. *Aust Endod J.* 2024;50:40–51. <https://doi.org/10.1111/aej.12805>